electronic reprint

Acta Crystallographica Section F
Structural Biology and Crystallization Communications
ISSN 1744-3091
Editors: **H. M. Einspahr and J. M. Guss**

Crystallization and preliminary X-ray analysis of *Escherichia coli* RNase HI–dsRNA complexes

Lioudmila V. Loukachevitch and Martin Egli

Acta Crystallographica Section F
Structural Biology and Crystallization Communications
ISSN 1744-3091

Crystallization and preliminary X-ray analysis of *Escherichia coli* RNase HI–dsRNA complexes

Lioudmila V. Loukachevitch and Martin Egli*

Department of Biochemistry, School of Medicine, Vanderbilt University, Nashville, Tennessee 37232, USA

Correspondence e-mail: martin.egli@vanderbilt.edu

Received 7 November 2006
Accepted 20 December 2006

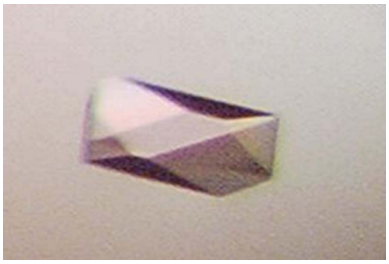

RNase H binds RNA–DNA hybrid and double-stranded RNA (dsRNA) duplexes with similar affinity, but only cleaves the RNA in the former. To potentially gain insight into the conformational origins of substrate recognition by the enzyme from *Escherichia coli*, cocrystallization experiments were carried out with RNase HI–dsRNA (enzyme–inhibitor) complexes. Crystals were obtained of two complexes containing 9-mer and 10-mer RNA duplexes that diffracted X-rays to 3.5 and 4 Å resolution, respectively.

1. Introduction

Ribonucleases H (RNases H) recognize hybrid duplexes between RNA and DNA and specifically cleave the RNA strand (Hostomsky *et al.*, 1993). The enzyme is thought to play a role in DNA replication and regulation of transcription. In *Drosophila*, RNase H1 is essential for development but not for proliferation (Filippov *et al.*, 1997, 2001). The work of Filippov and coworkers represents the first loss-of-function mutation in an *rnase H1* gene of a metazoan organism; none of the previously studied mutations in *rnase H* genes from either prokaryotes or lower eukaryotes were lethal. In addition, two genes encoding functional RNase H were determined to be essential for growth in *Bacillus subtilis* 168 (Itaya *et al.*, 1999). RNase H is also believed to be an important determinant for potent antisense activity by artificial oligonucleotides (Walder & Walder, 1988; Crooke, 1998). However, most chemically modified antisense oligonucleotides (AONs) do not elicit RNase H action, with the first-generation phosphorothioate DNA (PS-DNA; Crooke, 1995) and 2′-deoxy-2′-fluoroarabinonucleic acid (2′-FANA; Damha *et al.*, 1998) constituting exceptions. For example, AONs bearing 2′ modifications at the carbohydrate moiety bound to complementary RNA are not recognized as substrates by RNase H (Cook, 1998; Manoharan, 1999). Moreover, there are some observations based on treatment of human cell lines with antisense PS-DNAs that cast doubt on the role of RNase H as a major player in AON-mediated degradation of target mRNAs (ten Asbroek *et al.*, 2002). Thus, RNase H activity does not simply correspond to the activity assayed *in vitro*, but appears to be modulated by cell-type specific factors that could, for example, affect enzyme localization.

RNase HI from *Escherichia coli* is the best characterized bacterial RNase H (Kanaya & Crouch, 1983). The enzyme not only binds and processes RNA–DNA hybrids, but also exhibits considerable affinity for both RNA and DNA duplexes and to a lesser extent for single-stranded oligonucleotides. Thus, RNase H binds RNA–DNA and RNA duplexes ∼60-fold more strongly than DNA duplexes and ∼300-fold more strongly than single strands (Lima & Crooke, 1997). The K_d for the complex with a 17-mer dsRNA is ∼1 μ*M*. The crystal structure of the enzyme alone was determined many years ago (Katayanagi *et al.*, 1990; Yang, Hendrickson, Crouch *et al.*, 1990). However, no structure of a complex between *E. coli* RNase HI and a substrate duplex has been reported to date, although attempts have been made in this direction (Ishikawa *et al.*, 1991). The interactions between RNase H and heteroduplexes composed of DNA or chemically modified AONs and RNA have been the focus of numerous investigations over the years (Nakamura *et al.*, 1991;

Fedoroff *et al.*, 1993; Lima *et al.*, 1997, 2004; Minasov *et al.*, 2000; Sarafianos *et al.*, 2001; Yazbeck *et al.*, 2002). Early models of an enzyme–substrate complex were based on the assumption that the presence of 2′-hydroxyl groups in the RNA strand and the lack thereof in the DNA would be used by the enzyme to discriminate between RNA–DNA and dsRNA (Nakamura *et al.*, 1991). The mystery of how the enzyme can discriminate between hybrids and dsRNA is complicated by the fact that hybrid duplexes can adopt a variety of conformations, including the canonical A-form (Egli *et al.*, 1993; Ban *et al.*, 1994; Horton & Finzel, 1996; Sarafianos *et al.*, 2001). An NMR investigation of a hybrid duplex in solution provided evidence that the sugars of the DNA strand adopted the O4′-*endo* (Eastern) pucker (Fedoroff *et al.*, 1993). This particular conformation of the sugars results in a narrowing of the minor groove compared with dsRNA with A-form geometry. In the structure of HIV-1 reverse transcriptase in complex with a polypurine tract RNA–DNA the minor groove is indeed contracted, but 2′-deoxyriboses in the section of the duplex that is contacted by the RNase H domain adopt Southern-type puckers (Sarafianos *et al.*, 2001). In addition, the crystal structure of the complex between a bacterial RNase H and an RNA–DNA hybrid revealed that riboses adopt the C3′-*endo* pucker and 2′-deoxyriboses adopt C2′-*endo* or C1′-*exo* puckers (Nowotny *et al.*, 2005). Interestingly, the minor groove of the hybrid duplex in this structure is narrowed compared with the canonical A-form and five RNA 2′-hydroxyl groups are contacted directly by the enzyme.

A complete understanding of the substrate-specificity of RNase H will require analyses of its complexes with both RNA–DNA (substrate) and dsRNA (inhibitor). No structure of an inhibitor complex (RNase H–dsRNA) is available at present. In addition, the interpretation of the large amount of functional data with regard to the dependence of *E. coli* or human RNase H cleavage activity on location and nature of chemical modifications in the DNA strand (Lima *et al.*, 2004) would greatly benefit from the three-dimensional structures of enzyme–substrate and enzyme–inhibitor complexes. Our recent investigation of the conformational preferences of DNA duplexes with incorporated 2′-FANA residues provided evidence that this analog is unable to adopt a Southern pucker (Li *et al.*, 2006). This observation begs the following questions: (i) does the enzyme tolerate a limited range of conformations of the DNA or AON strand paired to RNA? and (ii) is the minor-groove width really the central recognition feature exploited by RNase H for substrate recognition?

The advent of RNA interference and the identification of the argonaute 2 (Ago2) enzyme that is responsible for the cleavage of mRNA targeted by miRNAs and siRNAs (Liu *et al.*, 2004; Meister *et al.*, 2004) provides further motivation for gaining an improved understanding of the conformational bases of substrate recognition by RNase H. The PIWI domain that forms part of the Ago2 enzyme adopts an RNase H fold (Song *et al.*, 2004; Ma *et al.*, 2005; Parker *et al.*, 2005) and yet is responsible for cleavage of dsRNA. In this context, it is also interesting to mention that the recently characterized RNase HI from the thermoacidophilic archaeon *Sulfolobus tokodaii* possesses both dsRNase and RNase H activity (Ohtani *et al.*, 2004).

In order to potentially gain insight into the structural origins of the ability of *E. coli* RNase to discriminate between RNA–DNA and dsRNA, we first directed our efforts towards the crystallization of enzyme–inhibitor (RNase HI–dsRNA) complexes. The decision to tackle the complex with RNA was partly a consequence of the notion that no particular precautions (*i.e.* use of inactive mutant proteins or Mg^{2+}-free crystallization buffers) would be necessary to prevent cleavage of dsRNAs, something that would be likely to hamper crystallization of the complex between wt-RNase HI and native RNA–DNA substrate. Cocrystallization of a protein with nonspecific nucleic acid sequences has the disadvantage that a strategy that combines a recognition sequence with a variety of sequences in the flanks cannot be pursued. Thus, numerous structural studies have concentrated on proteins bound to their specific DNA and RNA sequences. Conversely, relatively few structures have been determined for complexes that do not involve sequence-specific interactions (for examples, see Luger *et al.*, 1997; Ryter & Schultz, 1998; Viadiu *et al.*, 2000). Here, we report the crystallization of two different *E. coli* RNase HI–dsRNA complexes and the results of the data collection and preliminary crystallographic analysis of these complexes.

Table 1
RNA oligonucleotide sequences employed in the crystallization trials.

Code	Length	5′→3′ sequence
SC	15	GGA CUG AUC AGU CCA
Y	15	CAC UUG ACC UGG CUC
R	15	GAG CCA GGU CAA GUG
Y1	17	G CAC UUG ACC UGG CUC G
R1	17	C GAG CCA GGU CAA GUG C
Y2	16	G CAC UUG ACC UGG CUC
R2	16	C GAG CCA GGU CAA GUG
Y3	16	CAC UUG ACC UGG CUC G
R3	16	GAG CCA GGU CAA GUG C
Y4	9	CCU GGC UCG
R4	9	CGA GCC AGG
Y5	9	CUG GCU CGC
R5	9	GCG AGC CAG
Y6	10	GCA CUU GAC C
R6	10	GGU CAA GUG C

2. Materials and methods

2.1. Cloning, protein expression and purification

To prepare large amounts of *E. coli* RNase HI, the corresponding cDNA was cloned into the pET-29b expression vector with a TGA STOP codon followed by the GTT codon for C-terminal valine. Overexpression of RNase HI was performed in the *E. coli* BL21 (DE3) strain according to a standard protocol for expression with the pET-29b vector (Novagen). Briefly, transformed *E. coli* cells were grown in 2×YT media to an OD_{600} of 1.0 at 310 K and expression was induced with 1 m*M* IPTG. Cells were harvested by centrifugation after 3.5 h of cultivation at 310 K and the cell pellet was either used immediately for RNase HI isolation or was stored at 253 K. RNase HI was purified using DEAE-52 and P-11 columns according to published procedures (Kanaya & Crouch, 1983; Kanaya *et al.*, 1989; Yang, Hendrickson, Kalman *et al.*, 1990).

2.2. RNA synthesis and purification

All RNA oligonucleotides were purchased from Dharmacon Inc. (West Lafayette, CO, USA) and were PAGE-purified, deprotected and desalted.

2.3. Crystallization experiments

Our efforts to crystallize an *E. coli* RNase HI–dsRNA complex were based on the assumption that it was possible to identify an RNA duplex with just the right length and sequence to trap the complex in a well packed crystal lattice. Crystallization experiments were conducted using commercially available sparse-matrix screens (Jancarik & Kim, 1991; Berger *et al.*, 1996; Hampton Research, Aliso Viejo, CA, USA) and 'home-made' crystallization buffers. To date, we have included some 25 different RNA duplexes based on 15

oligoribonucleotides of various lengths and sequences in the trials (Table 1; different Y and R RNAs can be combined). Light scattering was routinely used to establish whether solutions of the complexes were monodisperse. In addition to screening crystallization conditions with the various RNase HI–dsRNA complexes, we also produced setups with protein and RNAs alone under identical conditions. Thus, crystals of wt-RNase H were grown from 20 m*M* HEPES pH 8.0, 16% PEG 3350 (Yang, Hendrickson, Kalman *et al.*, 1990; Fig. 1*a*). In many cases, crystals were obtained from RNA alone (Fig. 1*b*) and in some cases these crystals diffracted to atomic resolution, but structure determination was not further pursued.

An adapted gel-electrophoretic assay (Su *et al.*, 1994) that allows simultaneous detection of positively charged (protein) and negatively charged species (RNA) at a specific pH was employed to confirm that crystals contained both RNase HI and dsRNA. The pH of the running buffer for the single gel with central wells was kept at ∼6.7 so that RNA and protein migrated to the anode and cathode, respectively (Fig. 2). Crystals obtained from droplets containing RNase HI and dsRNA were thoroughly washed, dissolved and run on a 4.6% agarose gel that was first stained with ethidium bromide and then with Coomassie G250 (Bio-Rad) to detect RNA and protein, respectively. This particular method does not permit determination of the stoichiometry of the complex in the crystals.

By screening a variety of RNA duplexes (9-mers to 17-mers with either blunt ends or overhangs; Table 1), crystals of complexes were obtained with a variety of dsRNAs. However, they often did not diffract X-rays or only diffracted to low resolution. For example, crystals of the complex with the 15-mer RNA duplex Y–R (Fig. 1*c*, Table 1) diffracted to 7 Å and data of similar resolution were obtained for the complex with RNA duplex Y3–R2 (Table 1). The complex with RNA Y4–R4 diffracted to ∼10 Å. To date, the best crystals of complexes with *E. coli* RNase HI were obtained with RNA duplexes Y5–R5 (9-mer, complex 1) and Y6–R6 (10-mer, complex 2; Fig. 2*d*). Crystals of complex 1 and complex 2 were grown using the sitting-drop vapor-diffusion method. The concentrations of the complexes were 0.11–0.15 m*M*. Either 1 or 2 µl of complex were combined with 1 or 2 µl 50 m*M* bis-tris pH 6.1, 12.5% PEG 3350, 25 m*M* NaCl, 2 m*M* $MgCl_2$ and 1 m*M* TCEP. 4 µl 20 m*M* HEPES pH 8.0, 16% PEG 3350 was added to the drop containing complex 2 and reservoir solution.

Table 2
Selected crystal data and diffraction data statistics.

Data were collected on the 5-ID beamline at APS and were processed using the program *AUTOMAR* (Bartels & Klein, 2003). Values in parentheses are for the outer resolution shell.

	Complex 1	Complex 2
Protein	*E. coli* RNase HI	*E. coli* RNase HI
RNA duplex	CUG GCU CGC (Y5) GCG AGC CAG (R5)	GCA CUU GAC C (Y6) GGU CAA GUG C (R6)
CCD detector	MAR Mosaic 225	MAR Mosaic 225
Wavelength (Å)	1.000	1.000
Space group	$P2_1$	$P2_12_12_1$
Unit-cell parameters		
a (Å)	42.13	68.10
b (Å)	61.42	78.19
c (Å)	121.28	106.63
β (°)	93.16	—
Resolution range (Å)	30.0–3.50 (3.62–3.50)	30.0–3.99 (4.14–3.99)
Observations	36900	25887
Unique reflections	7476 (739)	5099 (490)
Completeness (%)	91.3 (94.6)	98.6 (95.4)
R_{merge}	0.102 (0.359)	0.061 (0.202)

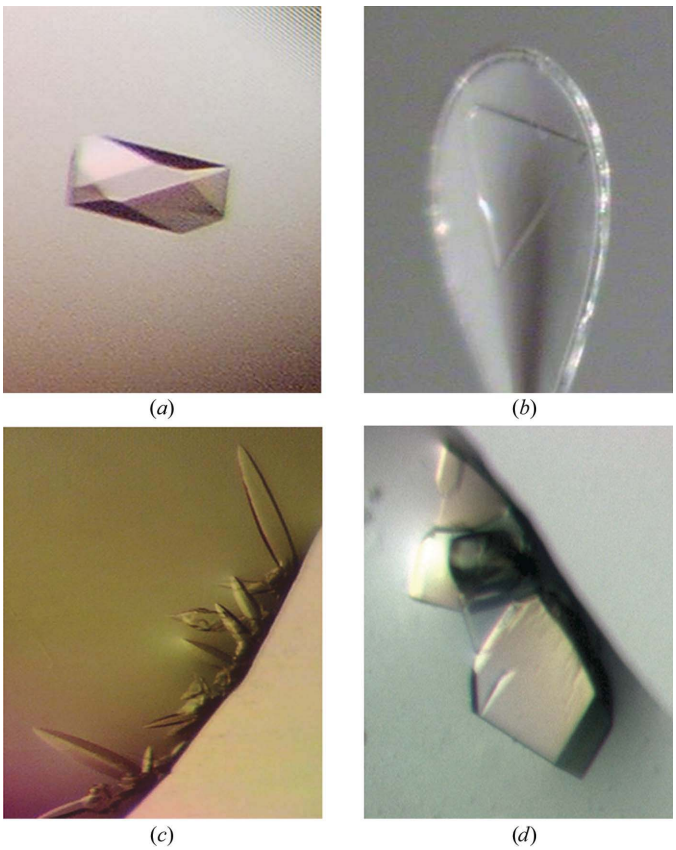

Figure 1
Micrographs of crystals. (*a*) wt-RNase HI (*E. coli*); (*b*) RNA duplex (CAC UUG ACC UGG CUC)–(GAG CCA GGU CAA GUG) (Y–R in Table 1), diffraction limit ∼2.1 Å; (*c*) complex between RNase HI and RNA duplex Y–R; (*d*) complex between RNase HI and RNA duplex (GCA CUU GAC C)–(GGU CAA GUG C) (Y6–R6 in Table 1).

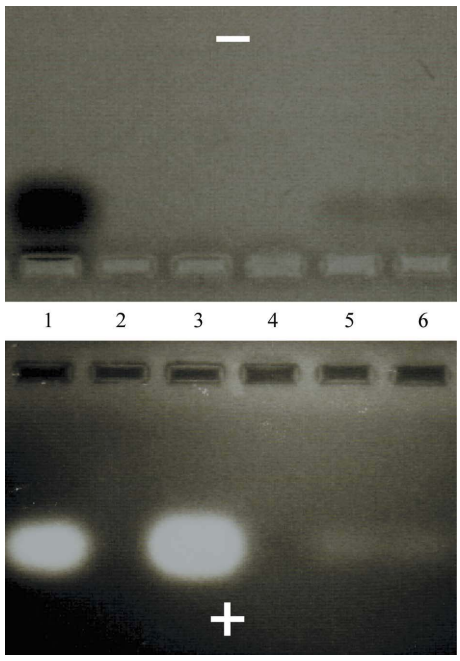

Figure 2
Gel-electrophoretic assay to establish the presence of both dsRNA (bottom panel) and *E. coli* RNase HI (top panel) in crystals: RNA and protein mixed in a 1:1 ratio (lane 1), RNA alone (lane 3) and two different crystals containing both RNase H and the RNA duplex Y–R (Table 1).

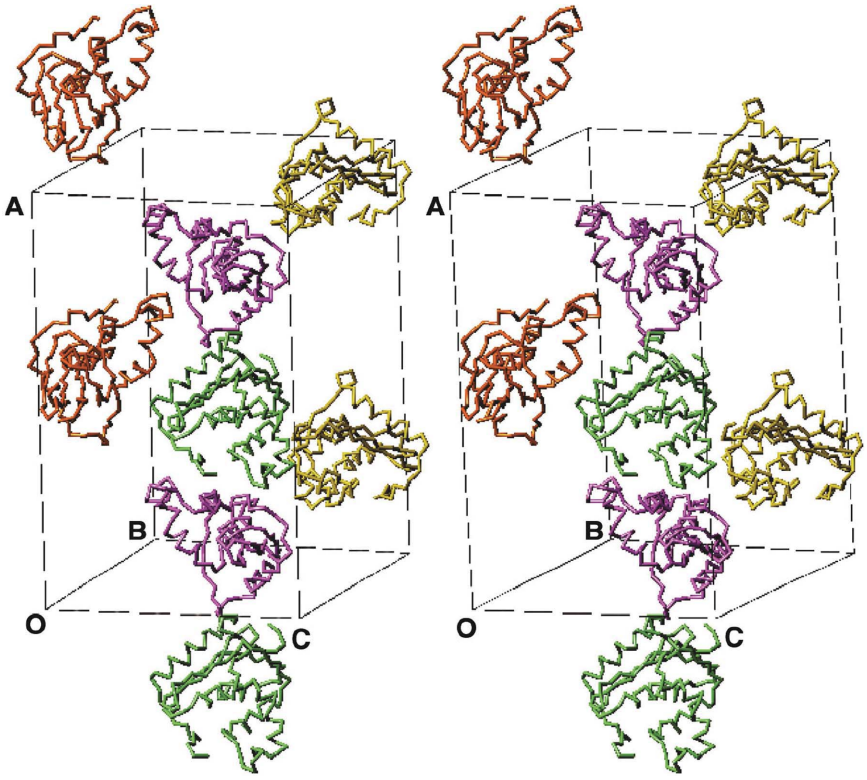

Figure 3
Stereo diagram of the crystallographic unit cell of complex 2 between *E. coli* RNase HI and RNA duplex (GCA CUU GAC C)–(GGU CAA GUG C) (Y6–R6; Table 1). Only the locations of protein molecules (two copies per crystallographic asymmetric unit, space group $P2_12_12_1$) are shown. There is sufficient space to accommodate two RNA duplexes per asymmetric unit.

2.4. Diffraction data collection and preliminary crystallographic analysis

Crystals were mounted in nylon loops using an initial cryoprotection protocol and screened for diffraction quality either on an in-house rotating-anode X-ray setup or at the Advanced Photon Source (APS), Argonne National Laboratory, Argonne, IL, USA (5-ID beamline, DND-CAT, Sector 5). The cryoprotection protocol for complex 1 and complex 2 was as follows. Crystals were cryoprotected with 30%(*v*/*v*) ethylene glycol, 12%(*w*/*v*) PEG 20 000, 30 m*M* bis-tris pH 6.1, 15 m*M* NaCl, 0.5 m*M* $MgCl_2$ and 1 m*M* TCEP.

A summary of selected crystal data and diffraction data statistics for the two crystals is given in Table 2. Crystals of complexes 1 and 2 diffracted to maximum resolutions of 3.5 and 3.99 Å, respectively. Unit-cell volume considerations indicated that complex 1 and 2 crystals could contain either one or two copies of a 1:1 RNase HI–dsRNA complex per crystallographic asymmetric unit (ASU) or alternatively could contain two copies of the dsRNA and a single copy of the protein or two copies of the protein and a single copy of the RNA. The values of the Matthews coefficient V_M (Matthews, 1968) for complex 1 crystals based on the above scenarios range between 6.84 $Å^3$ Da^{-1} (single copy of 1:1 complex, 82.0% solvent content) and 3.42 $Å^3$ Da^{-1} (two copies of 1:1 complex, 64.0% solvent content). In the case of complex 2 crystals, the corresponding values range between 6.04 $Å^3$ Da^{-1} (79.6% solvent content) and 3.02 $Å^3$ Da^{-1} (solvent content 59.3%).

Molecular-replacement searches in *CNS* (Brünger *et al.*, 1998) using the structure of wt-RNase HI from *E. coli* (PDB code 2rn2; Katayanagi *et al.*, 1992) as a search model indicate the presence of two protein molecules per ASU for both complex 1 and complex 2 crystals (Fig. 3). In both cases, this leaves ample space to accommodate either one or two RNA duplexes. However, the electron density in the regions presumably occupied by the RNAs after rigid-body and positional and *B*-factor refinements of the protein molecules alone is relatively weak. The lack of clear density at this stage may be a sign of high mobility of the RNA duplexes.

3. Conclusions

By conducting crystallization experiments with some 25 different *E. coli* RNase HI–dsRNA complexes, we have identified crystals of two complexes with 9-mer and 10-mer RNA duplexes that diffract X-rays to medium resolution. In both cases, the asymmetric unit appears to contain two enzyme molecules and one or perhaps two RNA duplexes. Further analysis of the crystal structures will reveal whether the resolution is sufficient to gain insight into the origins of the inability of RNase HI to process dsRNA. Inclusion of a larger number of RNA constructs in the crystallization trials can be expected to yield crystals that diffract X-rays to <3 Å.

This research was supported by US National Institutes of Health grant R01 GM55237. We thank Drs Walt Lima, Isis Pharmaceuticals Inc., Carlsbad, CA and Muthiah Manoharan, Alnylam Pharmaceuticals, Cambridge, MA for discussions and Drs Zdzislaw Wawrzak and Adriana Irimia for help with data collection and molecular replacement, respectively. Use of the Advanced Photon Source was supported by the US Department of Energy, Basic Energy Sciences, Office of Science under Contract No. W-31-109-Eng-38. The DuPont–Northwestern–Dow Collaborative Access Team (DND-CAT) Synchrotron Research Center at the Advanced Photon Source

(Sector 5) is supported by E. I. DuPont de Nemours & Co., The Dow Chemical Company, the National Science Foundation and the State of Illinois.

References

Ban, C., Ramakrishnan, B. & Sundaralingam, M. (1994). *J. Mol. Biol.* **236**, 275–285.

Bartels, K. S. & Klein, C. (2003). *AUTOMAR* version 3.04-0. MAR Research GmbH, Norderstedt, Germany.

Berger, I., Kang, C. H., Sinha, N., Wolters, M. & Rich, A. (1996). *Acta Cryst.* D**52**, 465–468.

Brünger, A. T., Adams, P. D., Clore, G. M., DeLano, W. L., Gros, P., Grosse-Kunstleve, R. W., Jiang, J.-S., Kuszewski, J., Nilges, M., Pannu, N. S., Read, R. J., Rice, L. M., Simonson, T. & Warren, G. L. (1998). *Acta Cryst.* D**54**, 905–921.

Cook, P. D. (1998). *Annu. Rep. Med. Chem.* **33**, 313–325.

Crooke, S. T. (1995). *Therapeutic Applications of Oligonucleotides*, pp. 63–79. Austin, TX, USA: R. G. Landes.

Crooke, S. T. (1998). Editor. *Antisense Research and Application*, pp. 1–50. Berlin: Springer.

Damha, M. J., Wilds, C. J., Noronha, A., Brukner, I., Borkow, G., Arion, D. & Parniak, M. A. (1998). *J. Am. Chem. Soc.* **120**, 12976–12977.

Egli, M., Usman, N. & Rich, A. (1993). *Biochemistry*, **32**, 3221–3237.

Fedoroff, O. Y., Salazar, M. & Reid, B. R. (1993). *J. Mol. Biol.* **233**, 509–523.

Filippov, V., Filippova, M. & Gill, S. S. (1997). *Biochem. Biophys. Res. Commun.* **240**, 844–849.

Filippov, V., Filippova, M. & Gill, S. S. (2001). *Mol. Genet. Genomics*, **265**, 771–777.

Horton, N. C. & Finzel, B. C. (1996). *J. Mol. Biol.* **264**, 521–533.

Hostomsky, Z., Hostomska, Z. & Matthews, D. A. (1993). *Nucleases*, 2nd ed., edited by S. M. Linn, S. R. Lloyd & R. J. Roberts, pp. 341–376. Cold Spring Harbor, NY, USA: Cold Spring Harbor Laboratory Press.

Ishikawa, M., Oda, Y., Katayanagi, K., Iwai, S., Ohtsuka, E. & Morikawa, K. (1991). *Nucleic Acids Res. Symp. Ser.* **24**, 253.

Itaya, M., Omori, A., Kanaya, S., Crouch, R. J., Tanaka, T. & Kondo, K. (1999). *J. Bacteriol.* **181**, 2118–2123.

Jancarik, J. & Kim, S.-H. (1991). *J. Appl. Cryst.* **24**, 409–411.

Kanaya, S. & Crouch, R. J. (1983). *J. Biol. Chem.* **258**, 1276–1281.

Kanaya, S., Kohara, A., Miyagawa, M., Matsuzaki, T., Morikawa, K. & Ikehara, M. (1989). *J. Biol. Chem.* **264**, 11546–11549.

Katayanagi, K., Miyagawa, M., Matsushima, M., Ishikawa, M., Kanaya, S., Ikehara, M., Matsuzaki, T. & Morikawa, K. (1990). *Nature (London)*, **347**, 306–309.

Katayanagi, K., Miyagawa, M., Matsushima, M., Ishikawa, M., Kanaya, S., Nakamura, H., Ikehara, M., Matsuzaki, T. & Morikawa, K. (1992). *J. Mol. Biol.* **223**, 1029–1052.

Li, F., Sarkhel, S., Wilds, C. J., Wawrzak, Z., Prakash, T. P., Manoharan, M. & Egli, M. (2006). *Biochemistry*, **45**, 4141–4152.

Lima, W. F. & Crooke, S. T. (1997). *Biochemistry*, **36**, 390–398.

Lima, W. F., Mohan, V. & Crooke, S. T. (1997). *J. Biol. Chem.* **272**, 18191–18199.

Lima, W. F., Nichols, J. G., Wu, H., Prakash, T. P., Migawa, M. T., Wyrzykiewicz, T. K., Bhat, B. & Crooke, S. T. (2004). *J. Biol. Chem.* **279**, 36317–36326.

Liu, J., Carmell, M. A., Rivas, F. V., Marsden, C. G., Thomson, J. M., Song, J.-J., Hammond, S. M., Joshua-Tor, L. & Hannon, G. J. (2004). *Science*, **305**, 1437–1441.

Luger, K., Mäder, A. W., Richmond, R. K., Sargent, D. F. & Richmond, T. J. (1997). *Nature (London)*, **389**, 251–260.

Ma, J.-B., Yuan, Y.-R., Meister, G., Pei, Y., Tuschl, T. & Patel, D. J. (2005). *Nature (London)*, **434**, 666–670.

Manoharan, M. (1999). *Biochim. Biophys. Acta*, **1489**, 117–130.

Matthews, B. W. (1968). *J. Mol. Biol.* **33**, 491–497.

Meister, G., Landthaler, M., Patkaniowska, A., Dorsett, Y., Teng, G. & Tuschl, T. (2004). *Mol. Cell*, **15**, 185–197.

Minasov, G., Teplova, M., Nielsen, P., Wengel, J. & Egli, M. (2000). *Biochemistry*, **39**, 3525–3532.

Nakamura, H., Oda, Y., Iwai, S., Inoue, H., Ohtsuka, E., Kanaya, S., Kimura, S., Katsuda, C., Katayanagi, K., Morikawa, K., Miyashiro, H. & Ikehara, M. (1991). *Proc. Natl Acad. Sci. USA*, **88**, 11535–11539.

Nowotny, M., Gaidamakov, S. A., Crouch, R. J. & Yang, W. (2005). *Cell*, **121**, 1005–1016.

Ohtani, N., Yanagawa, H., Tomita, M. & Itaya, M. (2004). *Nucleic Acids Res.* **32**, 5809–5819.

Parker, J. S., Roe, S. M. & Barford, D. (2005). *Nature (London)*, **434**, 663–666.

Ryter, J. M. & Schultz, S. C. (1998). *EMBO J.* **17**, 7505–7513.

Sarafianos, S. G., Das, K., Tantillo, C., Clark, A. D. Jr, Ding, J., Whitcomb, J. M., Boyer, P. L., Hughes, S. H. & Arnold, E. (2001). *EMBO J.* **20**, 1449–1461.

Song, J.-J., Smith, S. K., Hannon, G. J. & Joshua-Tor, L. (2004). *Science*, **305**, 1434–1437.

Su, C., Wang, F., Ciolek, D. & Pan, Y.-C. E. (1994). *Anal. Biochem.* **223**, 93–98.

ten Asbroek, A. L., van Groenigen, M., Nooij, M. & Baas, F. (2002). *Eur. J. Biochem.* **269**, 583–592.

Viadiu, H., Kucera, R., Schildkraut, I. & Aggarwal, A. K. (2000). *J. Struct. Biol.* **130**, 81–85.

Walder, R. T. & Walder, J. A. (1988). *Proc. Natl Acad. Sci. USA*, **85**, 5011–5015.

Yang, W., Hendrickson, W. A., Crouch, R. J. & Satow, Y. (1990). *Science*, **249**, 1398–1405.

Yang, W., Hendrickson, W. A., Kalman, E. T. & Crouch, R. J. (1990). *J. Biol. Chem.* **265**, 13553–13559.

Yazbeck, D. R., Min, K.-L. & Dahma, M. J. (2002). *Nucleic Acids Res.* **30**, 3015–3025.